FAST MULTIPHOTON MICROFABRICATION OF FREEFORM POLYMER MICROSTRUCTURES BY SPATIOTEMPORAL FOCUSING AND PATTERNED GENERATION

Y.-C. Li,[a] L.-C. Cheng,[a] C.-H. Lien,[b] C.-Y. Chang,[a] W.-C. Yen,[c] and S.-J. Chen[b,*]

[a] Department of Photonics, National Cheng Kung University, Tainan 701, Taiwan
[b] Department of Engineering Science, National Cheng Kung University, Tainan 701, Taiwan
[c] Material & Electro-Optics Research Division, Chung-Shan Institute of Science Technology, Tao-Yuan 325, Taiwan

ABSTRACT

One of the limits of a conventional multiphoton microfabrication is its low throughput due to the sequential nature of scanning process. In this study, a multiphoton microfabrication system based on spatiotemporal focusing and patterned excitation has been developed to provide freeform polymer microstructures fast. The system integrates a 10 kHz repetition rate ultrafast amplifier featuring strong instantaneous peak power (maximum 400 μJ/pulse at 90 fs pulse width) with a digital micromirror device generating designed patterns at the focal plane. As the result, three-dimensional freeform polymer microstructures using Rose Bengal as the photoinitiator are created by sequentially stacking up two-dimensional (2D) structures layer-by-layer. The size of each 2D fabrication area can be larger than 100 × 100 μm^2. Compared with scanning process or fixed mask pattern generation, this approach provides two- or three-fold fabrication speed and freeform microstructures. Furthermore, the system is capable of optical sectioning the fabricated microstructures for providing 3D inspection.

Keywords: spatiotemporal focusing, multiphoton microfabrication, microstructure, patterned generation.

1. INTRODUCTION

Multiphoton excitation (MPE) microfabrication is one of the most popular three-dimensional (3D) microfabrication techniques, and has been under development for over twenty years. This technology encompasses a broad range of applications such as microfluidic systems [1], 3D optical storage devices [2], and photonic crystal structures [3]. Recently, photopolymerization based on MPE has also been developed to further improve fabrication resolution since it uses low molecular weight photoinitiators to trigger reactions and requires an optical energy threshold to initiate the polymerization process [4-6]. Because multiphoton absorption is confined to the focal volume, photopolymerized structures with the desired 3D submicron features can be created [7-10]. This approach not only allows the creation of structures beyond the capability of conventional single-photon lithography, but also provides greater spatial resolution than other 3D microfabrication techniques. As such, multiphoton photopolymerization has attracted widespread interest for its potential use in fabricating intrinsic 3D microstructures with sub-diffraction limited spatial resolution [7]. The utilization of a short pulse width and tight focusing are critical for inducing sufficient two-photon absorption (TPA) and for achieving high precision fabrication. Previously, femtosecond 3D microfabrication has been demonstrated in resin- [6,7,11,12], protein- [5], silica- [13], and metal-substrates [14,15]. In addition, photonic crystals have also been demonstrated to be photopolymerizable by TPA [16-18]. However, the major drawback of this approach is that it constructs 3D structures point-by-point rather than in parallel, as accomplished by photolithographic processing. As a result, TPA has very slow fabrication speed and is limited to laboratory investigation and prototype fabrication.

Recent studies have shown that using simultaneous spatial and temporal focusing techniques can provide widefield and axially-resolved multiphoton imaging [19-24]. The advantage of widefield multiphoton microscopy is that less time is required to capture one frame, enabling rapid frame rates for capturing dynamic events. With a high-speed, high-sensitivity camera and an ultrahigh peak power laser, an imaging rate of a few hundred frames per second can be achieved [25]. Furthermore, this microscopy setup can be modified as a high-throughput multiphoton microfabrication system for the micromachining of microfluidic channels and optically transparent materials with high aspect ratio

* E-mail: sheanjen@mail.ncku.edu.tw; Tel.: +886-6-2757575 ext. 63351; Fax: +886-6-2766549

features [26,27]. The spatiotemporal focusing technique uses a diffraction grating to separate frequencies spatially, and then recombines them on the focal plane of an objective lens. Only in that plane do the different frequency components overlap in phase and produce a short, high-peak power pulse, allowing effective MPE to occur. Further, depending on laser beam spot size and system magnification, the widefield and axially-resolved MPE can excite an entire area, which is a definite advantage compared with conventional point scanning MPE. Therefore, this technique provides a solution for high-speed MPE microfabrication and enables high-throughput manufacturing.

Previously, the spatiotemporal focusing technique with a fixed optical mask realized MPE microfabrication [28]. The mask was placed at the image-conjugate plane of the grating surface and the focal plane of the objective lens, and so any kind of 3D structure could be created by sequentially changing the optical mask layer-by-layer. However, the use of static optical masks limits fabrication speed and throughput; and since the light source is typically a Ti:sapphire (ti-sa) ultrafast oscillator, the fabrication area is further limited by the available peak power. In this study, in order to instantly generate 3D freeform polymer microstructures, a multiphoton microfabrication system based on spatiotemporal focusing and patterned excitation has been developed. This system incorporates a 10 kHz repetition rate ultrafast amplifier featuring strong instantaneous peak power (maximum 400 μJ/pulse at 90 fs pulse width) and a digital micromirror device (DMD) generating two-dimensional (2D) designed patterns on the focal plane. Since the diffraction grating was placed on the image-conjugate plane of the objective lens' focal plane, the DMD generates designed 2D intensity patterns on the grating surface. Moreover, the size of the pattern is scaled by the magnification of the system; hence, increasing feature size does not require sacrificing fabrication speed. 3D freeform trimethylolpropane triacrylate (TMPTA) polymer microstructures using Rose Bengal (RB) as the photoinitiator were created by sequentially superimposing 2D structures while translating the sample stage axially. This approach can provide a greater than three-order increase in fabrication speed as compared to conventional point scanning MPE. In contrast with holographic femtosecond laser processing [29], the system can simultaneously provide additional nonlinear optical images of the fabricated microstructures for real-time 3D inspection.

2. SAMPLE PREPARATION AND MICROFABRICATION SETUP

A. High-throughput Multiphoton Microfabrication System

Figure 1 illustrates a schematic of the developed high-throughput multiphoton microfabrication system based on spatiotemporal focusing and patterned excitation. Key components include a ti-sa ultrafast amplifier (Spitfire Pro., Newport, USA), an ultrafast oscillator (Tsunami, Newport, USA) as the seed beam of the amplifier, an upright optical microscope (Axio imager 2, Carl Zeiss, Germany), a triple-axis sample positioning stage (H101A ProScan^{TM}, Prior, UK), an Andor EMCCD camera (iXon^{EM}+ 885 EMCCD, Andor, UK), a DMD (PJU-2100, RoyalTek, USA), and a data acquisition (DAQ) card with a field-programmable gate array (FPGA) module (PCI-7831R, National Instruments, USA). The ultrafast amplifier has a maximum peak power of 400 μJ/pulse and a pulse width of 90 fs at an average power of 4.0 W and a repetition rate of 10 kHz. First, a half-wave plate and a polarizer adjust the polarization and power of the amplifier; then, the beam oblique incidents on the DMD chip, which is controlled by a digital light processing technique, and generates the designed fabrication pattern. Following this, a relay lens pair is used to adjust the size of the pattern in order to fill the grating surface. The pulsing beam is spatially dispersed via a grating with a ruling density of 1200 lines/mm, the incident angle of which can be adjusted to ensure the dispersion's central frequency follows the optical axis. A set of relay lenses was inserted to lengthen the beam path, allowing for active 2D wavefront correctors, such as deformable mirrors or spatial light modulators, to be inserted for adaptive optics corrections, which in turn modulate our temporal focusing technique to improve fabrication quality. Finally, the dispersed frequencies propagate through the 4*f* setup, comprising the collimating lens and the objective lens (EC Plan-NEOFLUAR 40X/ NA 1.3, Carl Zeiss, Germany), ultimately focusing on the focal plane of the objective lens. Due to the diffraction from the grating at an oblique incident angle of 69.4°, the laser beam attains an elliptical cross section with the two axes at 300 μm and 150 μm. By controlling the motorized stage in the *z*-axis via the FPGA, sequential 2D patterned MPE polymerizations at different depths can be quickly obtained. In addition, the system is equipped with both bright field and widefield multiphoton fluorescence optics, so white light or two-photon fluorescence images can be acquired during the fabrication process, which can be used as real-time diagnostics of the fabrication structures. The two-photon fluorescence images can be then rendered as a 3D image.

Refractive elements such as the objective and collimating lenses can induce additional group velocity dispersion into the overall system. To correct this issue, the amplifier's built-in prism pair was adjusted to approach the optimal

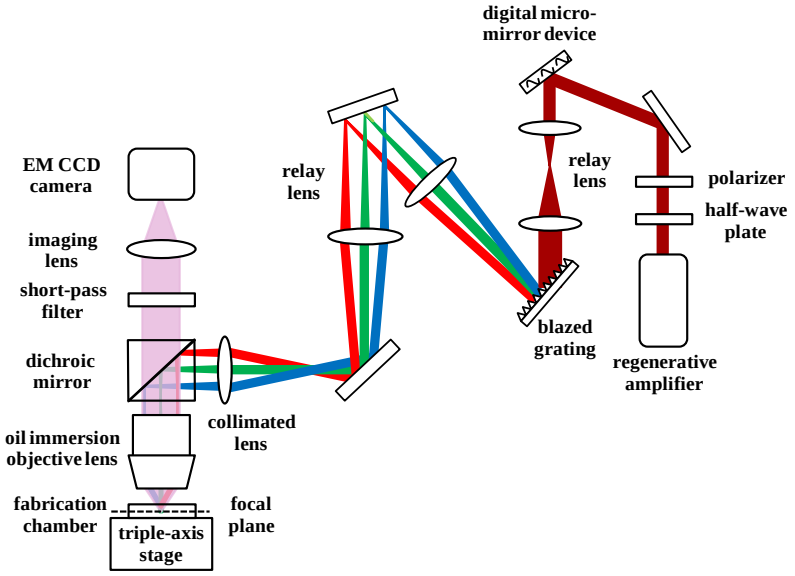

Fig. 1. Optical setup of the high-throughput multiphoton microfabrication system based on spatiotemporal focusing and patterned excitation.

pulse width (<120 fs); hence, temporal focusing efficiency for MPE polymerization can be enhanced, allowing for faster multiphoton microfabrication. Compared to holographic femtosecond laser processing [29], our system not only rapidly fabricates 3D freeform microstructures, but also provides fast optical sectioning. Patterned excitation is utilized for fabricating microstructures; however, uniform excitation is used to image the fabricated microstructures when the DMD is turned on. As a result, the contrast between the fabrication solution and the polymerized microstructures is sufficiently high [30], allowing for direct inspection of the microstructures during the fabrication procedure without washing out the fabrication solution or additional follow-up imaging.

B. Designing 3D Freeform Structures and Sample Preparation

In order to create 3D freeform microstructures with this microfabrication configuration, commercial CAD software such as AutoCAD, Pro/E, and Solidworks can be used to design any solid 3D structure. To transform 3D structures into 2D processing patterns, the 3D models were initially converted into STL format and saved as output files; then, the STL files were read by our LabVIEW code and converted into sequential 2D BMP files. Finally, the converted BMP files were read by another LabVIEW code that sequentially displays the sliced BMP patterns on a processing monitor. The DMD then synchronizes with the display patterns and generates patterned excitation on the focal plane of the objective lens.

A resin, ethoxylated TMPTA, was employed as the reactive monomer. The fabricated solution consisted of RB (Avocado Research Chemicals, UK) as the photoinitiator incorporated within a 0.1 M triethanolamine (TEA) co-initiator (Sigma-Aldrich, USA) solution, and mixed into a 75% (v/v) ethoxylated TMPTA (Sartomer, USA) solution. All chemicals and reagents were of analytical grade. According to our previous experimental results, the concentration of RB for 75% (v/v) TMPTA can be controlled at approximately 2.0 mM since a higher RB concentration is not necessary for the two-photon polymerization (TPP) process. Once completed, the 50 μl fabrication solution was confined in a small chamber created using a 50 μm-thick adhesive tape as a spacer to separate a 0.17 mm cover slip and the microscope slide. When fabricating, the structures were created from the bottom (slide) to top (slip) in order to prevent the incoming patterned excitation from being distorted by previous developed microstructures.

3. EXPERIMENTAL RESULTS AND DISCUSSIONS

A. System Calibrations

Microstructures can not be created when the laser dose is below the threshold fabrication energy for conventional scanning multiphoton microfabrication; on the other hand, microstructures could be damaged by a relatively high laser dose. Furthermore, it was found that a small pattern increases fabrication difficulty as compared with a larger one under

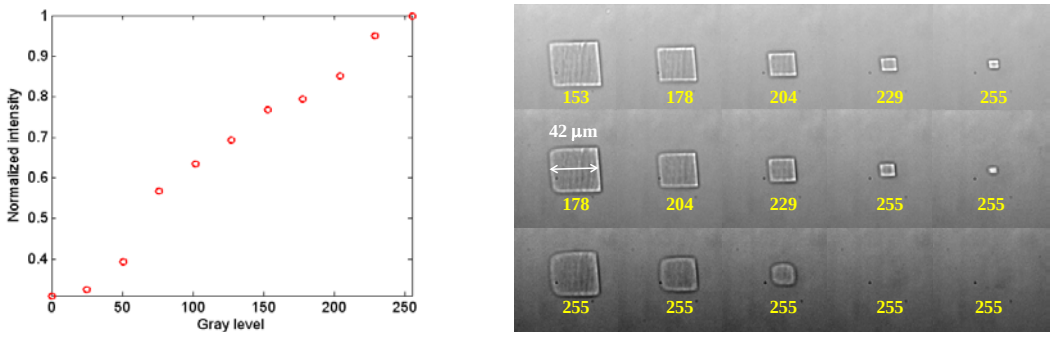

(a) (b)

Fig. 2. (a) Normalized TPEF intensities of fabricated solution as a function of different gray levels of the DMD. (b) Bright-field images of 5 different sizes of TMPTA polymer microstructures with the use of three different laser powers at 12.2 mW, 8.7 mW, and 5.2 mW (from top to bottom) corresponding to the minimum demanded gray levels, respectively. Sizes of the fabricated squares are respectively 42 µm, 33 µm, 23 µm, 14 µm, and 8 µm (from left to right).

the same laser dose incident on the DMD chip during the high-throughput microfabrication process. Herein, the same laser dose means that the same laser power is utilized with the same pulse width and pulse number. Consequently, a suitable laser dose to match the size of the 2D fabricated pattern should be investigated. The power of the ultrafast amplifier can not be rapidly changed; hence, the gray level of the DMD can be adopted to adjust the laser dose. Therefore, a dose-gray level relation was studied according to the ratio of the TPEF intensity (i.e. the laser excitation dose) to the gray level projected onto the DMD chip. The 0~255 gray levels represent the different “on” states for the 8-bit DMD, meaning that the DMD can act as a pulse selector to tune the pulse number on the fabricated pixel or area. For the 10 kHz ultrafast amplifier, a gray level of 255 represents 10,000 pulses per second, while a gray level of 128 refers to 5,000 pulses per second, and so on. Therefore, different gray levels for different sizes of fabricated patterns have been studied to further develop TMPTA polymer microstructures. Figure 2(a) shows the excitation of the normalized TPEF intensities of the fabricated solution as a function of different gray levels of the DMD. The TPEF intensity is nearly linearly proportional to the gray level, as shown in Fig. 2(a). Figure 2(b) illustrates that five different square pattern sizes can be fabricated with minimum gray levels of the DMD chip under the laser powers of 12.2 mW, 8.7 mW, and 5.2 mW (from top to bottom), respectively. The yellow numeral below each structure indicates the approximate minimum gray level required for fabrication under the three respective laser powers. The experimental results confirm that a larger pattern can be developed with a lower gray level (i.e. lower laser dose) under the proposed process. Interestingly, the first row of Fig. 2(b) demonstrates that although a suitable high laser power is provided, a higher gray level is required for a small pattern, while a lower gray level is needed for a larger pattern. Additionally, a low laser dose can prevent the fabricated microstructure from being damaged. However, if the laser power is insufficient, despite employing the highest gray level, microstructures can not be fabricated or their shapes will have slight deformations, as shown in the last row of Fig. 2(b).

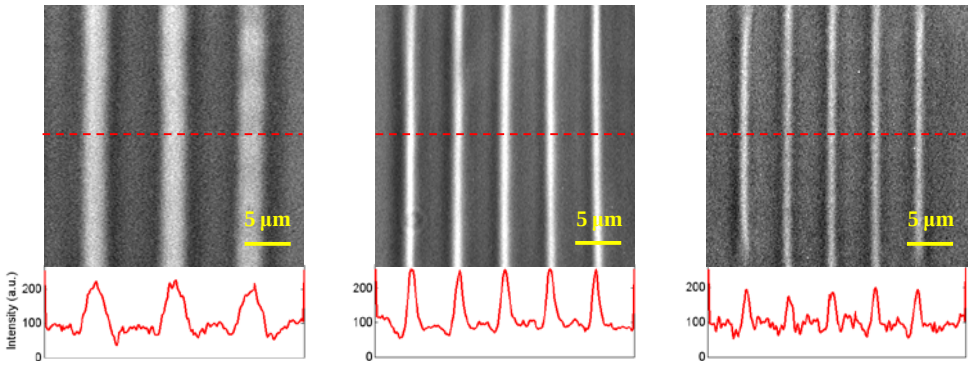

(a) (b) (c)

Fig. 3. Bright-field images and profiles of three stripes fabricated with pixel numbers of (a) 35, (b) 20, and (c) 5, respectively. The corresponding widths of the stripes are 3.8 µm, 1.6 µm, and 1 µm, respectively. The profiles correspond to the red dotted line in the bright-field images.

The lateral fabrication resolution of the high-throughput multiphoton microfabrication system is in need of clarification for further processing. A fabrication area of 76 μm × 43 μm under the system setup corresponds to the 640 × 360 pixel number of the DMD chip, indicating that 1 pixel corresponds to roughly 120 nm × 120 nm. Three stripe patterns with pixel numbers of 35, 20, and 5 were fabricated to examine the lateral resolution, the estimated sizes of which are around 4.2 μm, 2.4 μm, and 0.6 μm, respectively. However, Figs. 3(a), (b), & (c) show that the widths of the stripes are approximately 3.8 μm, 1.6 μm, and 1μm, respectively. In this regard, photopolymerization requires the threshold fabrication energy to initiate the process, and so actual fabricated sizes could be slightly smaller than the estimated size. As such, the stripes in Figs. 3(a) & (b) match expectations, but the width of the stripes in Fig. 3(c) is only 1 μm, which may stem from the diffraction limit and/or system distortions. Currently, the lateral fabrication resolution of the system is around 1 μm.

B. Fabrication and Inspection of Freeform Polymer Microstructures

For 3D freeform microfabrication, the sequential 2D bitmap files sliced from a designed 3D CAD model were downloaded into the LabVIEW program to sequentially implement the 2D pattern excitation via the DMD. The 2D TPP microstructures were sequentially formed on the focal plane based on spatiotemporal focusing and patterned excitation, and then stacked in a 3D polymer microstructure while translating the sample stage axially. The remaining fabrication solution was then washed with water. To sufficiently support the MPE photochemistry process in the fabrication solution, a laser power of at least a few mWs at the excitation time of around 1 second was adopted. Figure 4(a) shows a fabricated star structure with a feature size of around 30 μm under a laser power of 8.7 mW, an excitation time of 4/3 seconds, and a *z*-axis step of 1 μm. Unlike conventional scanning multiphoton microfabrication, the proposed system can increase feature size without sacrificing fabrication speed. Figures 4(b) & (c) demonstrate that bigger microstructures can be created using smaller magnifications of the optical system. The magnification for Fig. 4(a) is 40X; however, the magnifications for Figs. 4(b) & (c) were reduced to 20X and 10X, while the feature sizes were enlarged to 60 μm and 120 μm, respectively. The excitation areas were enlarged, so the laser powers were also increased to 12.2 mW and 15.7 mW for Figs. 4(b) & (c), respectively. The fabrication times of these three microstructures were equal, requiring only 40 seconds. Therefore, it is possible to increase the fabrication area by readjusting the magnification of the optical system, such as the objective lens and the relay lens pair in Fig. 1.

In addition to the above scale-up capability, the 3D renderings of the TPEF images of the excitation patterns can be viewed in real-time during the high-throughput microfabrication process, as shown in Fig. 5. The front-view bright-field images of the fabricated microstructures before rinsing the remaining solution are inserted in the 3D renderings. Figure 5(a) displays a 3D pyramid structure, where the base area is around 40 × 40 μm^2 while the height is 45 μm. The fabrication laser power was 7.5 mW, the excitation time was 4/3 seconds per layer, and the *z*-axis step was 1 μm. Figure 5(b) demonstrates that four different shaped structures with different heights can be fabricated simultaneously. The heights are 8μm, 12 μm, 16 μm, and 20 μm for the triangle, star, rectangle, and circle, respectively. The fabrication time for developing these microstructures is within 30 seconds.

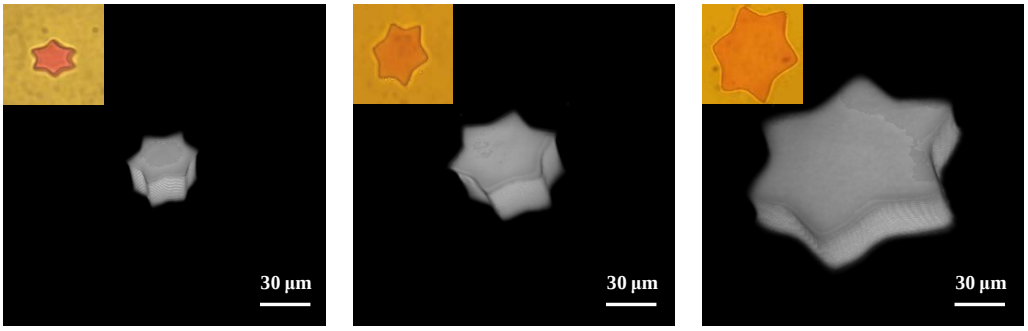

(a) (b) (c)

Fig. 4. TPEF images of different size microstructures created by different magnifications of the objective lenses at (a) 40X, (b) 20X, and (c) 10X. The heights of three structures are all 30 μm.

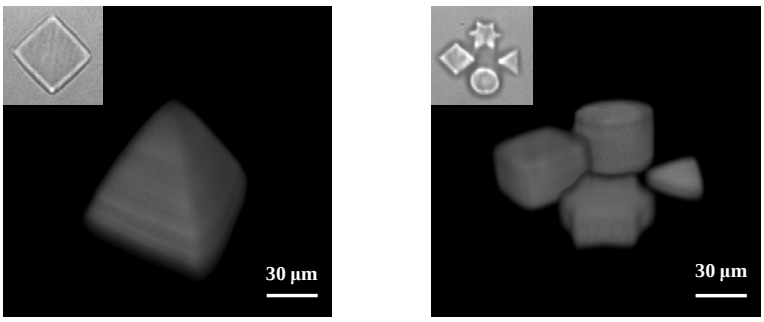

(a) (b)

Fig. 5. 3D renderings of the TPEF images of the excitation patterns during the high-throughput microfabrication process: (a) pyramid structure and (b) multiple objects (triangle, star, rectangle, and circle) with different heights. Inset: 2D front-view bright-field images.

After washing the remaining solution, the developed microstructures in Fig. 5(b) were imaged again using the multiphoton microfabrication system with only the widefield imaging function. Figure 6(a), and 6(b) show the 2D TPEF images of the developed microstructures where the positions are 15 μm, 10 μm high from the bottom of the structures. Fig. 6(c) shows the TPEF image at the bottom of the structures. The shapes in Fig. 6 are nearly identical to Fig. 5(b), thus providing further evidence that the TPEF images grabbed during the high-throughput fabrication process can be utilized as online diagnostics for fabricating microstructures. Therefore, the proposed system based on spatiotemporal focusing and patterned excitation not only provides high-throughput microfabrication, but also offers real-time optical sectioning for 3D online inspection. Compared with conventional point-scanning TPEF images, the images look somewhat blurry; nevertheless, according to our previous study [31], the image quality can be improved to achieve sub-micron resolution.

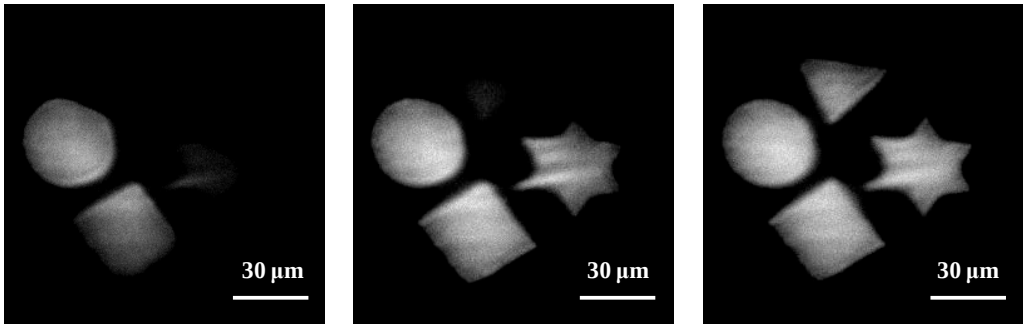

(a) (b) (c)

Fig. 6. 2D sectional TPEF images of the fabricated microstructures in Fig. 5(b) after washing the remaining solution: (a) 15μm high from the bottom of the structures and (b) 10 μm high from the bottom of the structures and (c) at the bottom of the structures.

4. CONCLUSIONS

A multiphoton microfabrication system based on spatiotemporal focusing and patterned excitation has been developed to enhance fabrication speed and also realize microfabrication of 3D freeform microstructures. 3D freeform polymer microstructures can be created by sequentially stacking 2D structures. The fabrication times for developing microstructures require less than one minute. Compared with conventional scanning MPE microfabrication, this approach provides an increase in fabrication speed of more than three-order, offering the possibility of mass-production, while simultaneously providing real-time optical sectioning for the fabricated microstructures. Therefore, the multiphoton microfabrication system not only provides the capability of high-throughput microfabrication, but also offers optical sectioning for 3D online inspection.

ACKNOWLEDGMENTS

This work was supported by the National Science Council (NSC) in Taiwan with the grant numbers of NSC 99-2627-B-006-017, NSC 99-3111-B-006-004, and NSC 100-2623-E-006-016-D.

REFERENCES

[1] M. Stoneman, M. Fox, C. Y. Zeng, and V. Raicu, "Real-time monitoring of two-photon photopolymerization for use in fabrication of microfluidic devices," Lab Chip **9**, 819–827 (2009).

[2] C. E. Olson, M. J. R. Previte, and J. T. Fourkas, "Efficient and robust multiphoton data storage in molecular glasses and highly crosslinked polymers," Nat. Materials **1**, 225–228 (2002).

[3] R. Guo, Z. Li, Z. Jiang, D. Yuan, W. Huang, and A. Xia, "Log-pile photonic crystal fabricated by two-photon photopolymerization," J. Optics A: Pure Appl. Opt. **7**, 396–399 (2005).

[4] C. R. Lambert, I. E. Kochevar, and R. W. Redmond, "Differential reactivity of upper triplet states produces wavelength-dependent two-photon photosensitization using Rose Bengal," J. Phys. Chem. B **103**, 3737–3741 (1999).

[5] J. D. Pitts, P. J. Campagnola, G. A. Epling, and S. L. Goodman, "Submicron multiphoton free-form fabrication of proteins and polymers: studies of reaction efficiencies and applications in sustained release," Macromolecules **33**, 1514–1523 (2000).

[6] P. J. Campagnola, D. M. Delguidice, G. A. Epling, K. D. Hoffacker, A. R. Howell, J. D. Pitts, and S. L. Goodman, "3-dimensional submicron polymerization of acrylamide by multiphoton excitation of xanthene dyes," Macromolecules **33**, 1511–1513 (2000).

[7] S. Kawata, H. B. Sun, T. Tanaka, and K. Takada, "Finer features for functional microdevices," Nature **412**, 697–698 (2001).

[8] W. Denk, J. H. Strickler, and W. W. Webb, "Two-photon laser scanning fluorescence microscopy," Science **248**, 73–76 (1990).

[9] T. Tanaka, H. B. Sun, and S. Kawata, "Rapid sub-diffraction-limit laser micro/nanoprocessing in a threshold material system," Appl. Phys. Lett. **80**, 312–314 (2002).

[10] M. Miwa, S. Juodkazis, T. Kawakami, S. Matsuo, and H. Misawa, "Femtosecond two-photon stereo-lithography," Appl. Phys. A: Mater. Sci. Process. **73**, 561–566 (2001).

[11] T. Watanabe, M. Akiyama, K. Totani, S. M. Kuebler, F. Stellacci, W. Wenseleers, K. Braun, S. R. Marder, and J. W. Perry, "Photoresponsive hydrogel microstructure fabricated by two-photon initiated Polymerization," Adv. Funct. Mater. **12**, 611–614 (2002).

[12] Z. B. Sun, X. Z. Dong, W. Q. Chen, S. Nakanishi, M. Duan, and S. Kawata, "Multicolor polymer nanocomposites: in situ synthesis and fabrication of 3D microstructures," Adv. Mater. **20**, 914–919 (2008).

[13] A. Marcinkevicius, S. Juodkazis, M. Watanabe, M. Miwa, S. Matsuo, and H. Misawa, "Femtosecond laser-assisted three-dimensional microfabrication in silica," Opt. Lett. **26**, 277–279 (2001).

[14] P. W. Wu, W. C. Cheng, I. B. Martini, B. Dunn, B. J. Schwartz, and E. Yablonovitch, "Two-photon photographic production of three-dimensional metallic structures within a dielectric matrix," Adv. Mater. **12**, 1438–1441 (2000).

[15] Y. Y. Cao, N. Takeyasu, T. Tanaka, X. M. Duan, and S. Kawata, "3D metallic nanostructure fabrication by surfactant-assisted multiphoton-induced reduction," Small **5**, 1144–1148 (2009).

[16] N. Takeshima, Y. Narita, T. Nagata, and S. Tanaka, "Fabrication of photonic crystals in ZnS-doped glass," Opt. Lett. **30**, 537–539 (2005)

[17] G. Zhou and M. Gu, "Direct optical fabrication of three-dimensional photonic crystals in a high refractive index $LiNbO_3$ crystal," Opt. Lett. **31**, 2783–2785 (2006).

[18] Z. B. Sun, X. Z. Dong, S. Nzkanishi, W. Q. Chen, X. M. Duan, and S. Kawata, "Log-pile photonic crystal of CdS-polymer nanocomposites fabricated by combination of two-photon polymerization and in situ synthesis," Appl. Phys. A **86**, 427–431 (2007).

[19] D. Oron, E. Tal, and Y. Silberberg, "Scanningless depth-resolved microscopy," Opt. Express **13**, 1468–1476 (2005).

[20] G. Zhu, J. V. Howe, M. Durst, W. Zipfel, and C. Xu, "Simultaneous spatial and temporal focusing of femtosecond pulses," Opt. Express **13**, 2153–2159 (2005).

[21] M.E. Durst, G. Zhu, and C. Xu, "Simultaneous spatial and temporal focusing in nonlinear microscopy," Opt. Commun. **281**, 1796–1805 (2008).

[22] A. Vaziri, J. Tang, H. Shroff, and C. V. Shank, "Multilayer three-dimensional super resolution imaging of thick biological samples," PNAS **105**, 20221–20226 (2008).

[23] E. Papagiakoumou, F. Anselmi, A. Bègue, V. deSars, J. Glückstad, E. Y. Isacoff, and V. Emiliani, "Scanless two-photon excitation of channelrhodopsin-2," Nat. Methods **7**, 848–854 (2010).
[24] O. D. Therrien, B. Aubé, S. Pagès, P. De Koninck, and D. Côté, "Wide-field multiphoton imaging of cellular dynamics in thick tissue by temporal focusing and patterned illumination," Biomed. Opt. Express **2**, 696–704 (2011).
[25] L.-C. Cheng, C.-Y. Chang, C.-Y. Lin, K.-C. Cho, W.-C. Yen, N.-S. Chang, C. Xu, C. Y. Dong, and S.-J. Chen, "Spatiotemporal focusing-based widefield multiphoton microscopy for fast optical sectioning," Opt. Express **20**, 8939–8948 (2012).
[26] F. He, H. Xu, Y. Cheng, J. Ni, H. Xiong, Z. Xu, K. Sugioka, and K. Midorikawa, "Fabrication of microfluidic channels with a circular cross section using spatiotemporally focused femtosecond laser pulses," Opt. Lett. **35**, 1106–1108 (2010).
[27] D. N. Vitek, D. E. Adams, A. Johnson, P. S. Tsai, S. Backus, C. G. Durfee, D. Kleinfeld, and J. A. Squier, "Temporally focused femtosecond laser pulses for low numerical aperture micromachining through optically transparent materials," Opt. Express **18**, 18086–18094 (2010).
[28] D. Kim and P. T. C. So, "High-throughput three-dimensional lithographic microfabrication," Opt. Lett. **35**, 1602–1604 (2010).
[29] S. Hasegawa and Y. Hayasaki, "Adaptive optimization of hologram in holographic femtosecond laser processing system," Opt. Lett. **34**, 22–24 (2009).
[30] C.-Y. Lin, C.-H. Lien, K.-C. Cho, C.-Y. Chang, N.-S. Chang, P. J. Campagnola, C. Y. Dong, and S.-J. Chen, "Investigation of two-photon excited fluorescence increment via crosslinked bovine serum albumin," Optics Express **20**, accepted (2012).
[31] C.-Y. Chang, L.-C. Cheng, H.-W. Su, K.-C. Cho, W.-C. Yen, C. Xu, C. Y. Dong, and S.-J. Chen, "Widefield multiphoton microscopy with image-based adaptive optics system," submitted for publication.